

Supporting Information for:

Modification with Heme proteins Increases the Diffusive Movement of Nanorods in Dilute Hydrogen Peroxide Solutions

Ada-Ioana Bunea^a, Ileana-Alexandra Pavel^a, Sorin David^a and Szilveszter Gáspár^{a*}

^aInternational Centre of Biodynamics, 1B Intrarea Portocalelor, 060101 – Bucharest, Romania

*corresponding author; Email: sgaspar@biodyn.ro

Contents

Materials.....	2
Fabrication of nanorods	2
Modification of nanorods with heme proteins	4
Colorimetric determination of peroxidase activity	5
Determination of the diffusion coefficient of the nanorods.....	5
Determination of the open circuit potential of the nanorod segments	7
Catalytic cycles of heme proteins.....	7
References.....	8

Materials

Porous alumina membranes (Catalog no. 6809-6022, with cylindrical pores of 200 nm in diameter) were purchased from Whatman. Metal plating solutions (Orotemp 24 and Platinum TP) were purchased from Italgalvano s.p.a.. Pyrrole (98%), pyrrole-2 carboxylic acid (99%), potassium chloride ($\geq 99\%$), 3-amino-1-propanethiol hydrochloride, N-(3-dimethylaminopropyl)-N'-ethylcarbodiimide hydrochloride (EDC), peroxidase from horseradish (HRP, catalog no. P8375), catalase from bovine liver (Cat, catalog no. C30), cytochrome C from bovine heart (Cyt c, $\geq 95\%$, catalog no. C2037) and ethanol were all purchased from Sigma-Aldrich. 3,3'-dithiodipropionic acid and N-hydroxysuccinimide (NHS, $\geq 97\%$) were purchased from Fluka. Copper(II) chloride dehydrate ($\geq 99\%$), 3,3',5,5'-tetramethylbenzidine ($\geq 98\%$), and hydrogen peroxide (30%) were purchased from Carl Roth GmbH. Methanol (≥ 99.9) was purchased from Emsure. Sodium hydroxide ($\geq 98\%$) was purchased from Lach-Ner. $\text{CuSO}_4 \cdot 5\text{H}_2\text{O}$ and HCl (37%) were from local providers.

Fabrication of nanorods

Pt-Au nanorods were fabricated by modifying a previously described procedure.¹ Porous alumina membranes were used as template for nanorod growth. A 400 nm thick sacrificial layer of Cu was deposited onto the branched side of these membranes by physical vapor deposition (using a PVD system from Kurt J. Lesker Company). This layer served as working electrode in the subsequent three electrodeposition steps carried out on a Model 1470E potentiostat from Solartron. In the first electrodeposition step, 15 C of additional sacrificial Cu were plated into the membrane at -0.9 V (vs. Ag/AgCl, 3M KCl) to fill the branched section of the pores. In the second electrodeposition step, the Au nanorod segment was grown using an applied potential of -0.9 V, 6 C of charge, and the Orotemp 24 plating solution mentioned under the Materials section. In the third electrodeposition step, the Pt nanorod segment was grown using a constant current of 1 mA / cm², 6 C of charge, and the Platinum TP plating solution also mentioned above. After these electrodeposition steps, the nanorod-filled membranes were immersed first into 0.5 M CuCl_2 in a 20% HCl aqueous solution (to dissolve the Cu sacrificial layer) and then into 5 M NaOH (to dissolve the alumina membrane). Then the nanorods were centrifuged and rinsed several times, and finally suspended into ultrapure water. The PPy segment (replacing the Pt from the above nanorods) was fabricated through the electrochemical copolymerization of pyrrole and 2-carboxy-pyrrole in a solution containing 120 mM pyrrole and 40 mM 2-carboxy-pyrrole (in a 1:1 mixture of 0.2 M KCl aqueous solution and methanol) and using 15 potential sweeps between 0 and 0.9 V vs. Ag/AgCl, 3 M KCl.

Figure 1S shows a picture of PPy-Au nanorods deposited onto glass from a suspension made in ultrapure water. The size distribution of the fabricated nanorods was determined using optical images as the one shown in Figure 1S, ImageJ² to determine particle size in pixels, and then a XY calibration of 0.08 μm

characterizing our microscope and camera system. Figure 2S shows typical length distributions for a batch of 1.5 μm long nanorods and a batch of 2.5 μm long nanorods.

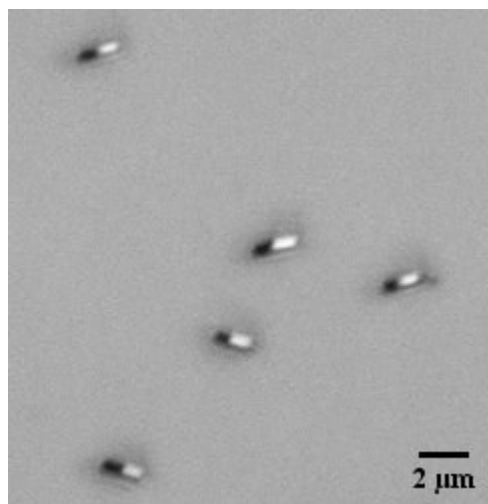


Figure 1S. Optical microscopy image of PPy-Au nanorods magnified 100 times, in reflected light mode. Observation: The Au segments appear bright (because reflect light) while the polymer segments are dark.

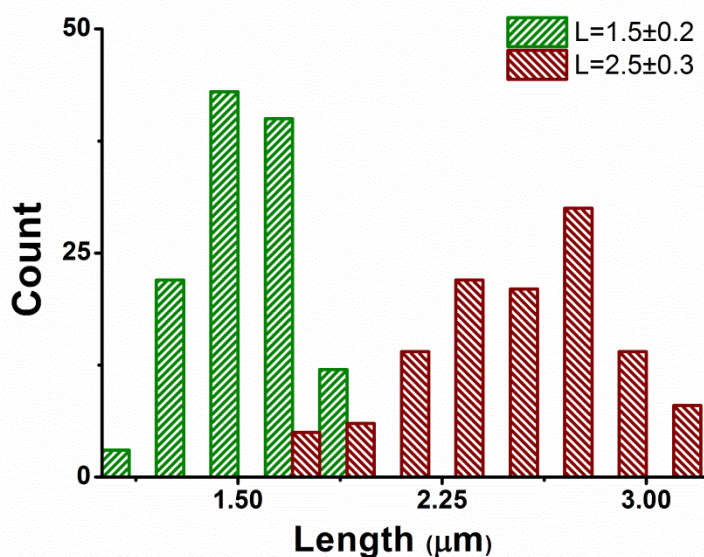


Figure 2S. Length histograms for the shortest and the longest nanorods used in our experiments. Observation: Shorter nanorods have a narrower size distribution.

The fabricated nanorods were also investigated using a Nanowizard II Atomic Force Microscope (AFM) from JPK Instruments AG. Figure 3S shows two typical AFM images of our hemeprotein-modified nanorods. They were obtained in intermittent contact-mode with an ArrowTM Silicon SPM Sensor (from Nano World AG, characterized by a resonance frequency of 285 kHz and a force constant of 42 N/m). The ratio between the set-point amplitude and the free amplitude of the AFM tip was set to 0.64-0.66. The AFM images confirm the length of our nanorods determined using optical microscopy. However, the diameter and into a much smaller extent also the height of the nanorods are distorted due to the combination of the tip and sample geometries (i.e. by convolution). Unfortunately, the nanorods had relatively featureless phase images (not shown).

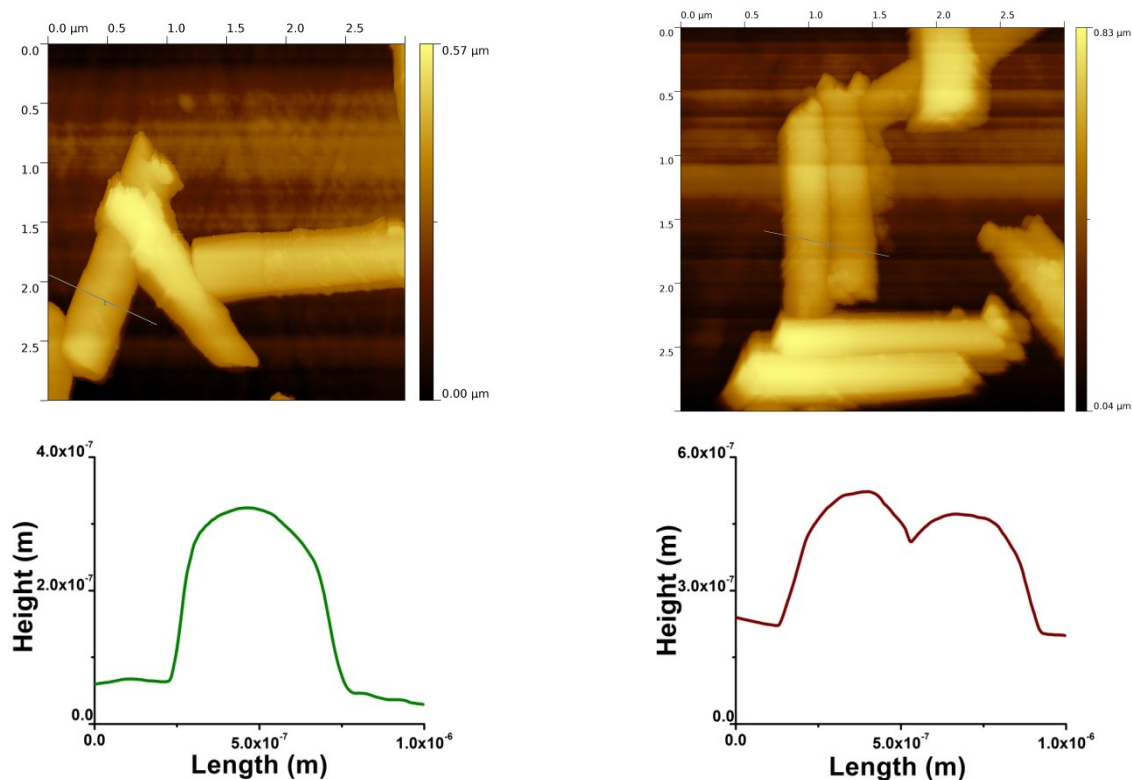


Figure 3S. Typical topography images obtained by intermittent contact-mode AFM (upper row) and profiles extracted from these topography images (lower row) for (HRP)PPy-Au(Cyt c) nanorods adsorbed onto a poly(propylene) substrate. Observation: Data was leveled by mean plane subtraction for the above images. No other processing was made.

Modification of nanorods with hemeproteins

Hemeprotein-modified nanorods will be denoted from now on as (Protein1)Segment1-Segment2(Protein2). For example, nanorods with HRP immobilized onto the PPy segment, and Cyt c immobilized onto the Au segment, will be denoted as (HRP)PPy-Au(Cyt c). In order to obtain such nanorods, PPy-Au nanorods were first incubated in a solution of 3-amino-1-propanethiol (10 mM in ethanol) for at least 12 hours. A monolayer displaying amino groups self-assembled onto the Au segment of the nanorods during this incubation. In the next step, the carboxyl groups of the PPy end of the nanorods were activated by dispersing the nanorods in a mixture of 200 mM EDC and 50 mM NHS for 7 minutes. The nanorods with activated carboxyl groups were washed once, and then immediately immersed into an HRP solution (0.1 mg/mL) for 1 hour. The resulting structures, (HRP)PPy-Au, were either tested in hydrogen peroxide or further modified with hemeproteins (after being washed free of unbound HRP). Cyt c or Cat was immobilized onto the Au segment covered with 3-amino-1-propanethiol by incubating the nanorods in a solution containing EDC (200 mM), NHS (50 mM) and the protein to be immobilized (0.1 mg/mL) for 1 hour. When building the (HRP)PPy-Au(HRP) structure, 3,3'-dithiodipropionic acid was used instead of 3-amino-1-propanethiol to form a monolayer displaying carboxyl groups onto the Au segment of the nanorods. The carboxyl groups from the PPy and the Au

segments were then simultaneously activated and used to immobilize HRP as described above for the PPy segment. The successful immobilization of hemeproteins was confirmed using colorimetric methods whenever possible (see Figure 4S and the next section). The successful immobilization of catalase onto the nanorods was tested by suspending the nanorods in hydrogen peroxide solution. Only nanorods with catalase produced oxygen bubbles visible to the naked eye, and only when these nanorods were suspended in concentrations of hydrogen peroxide higher than 1.5%.

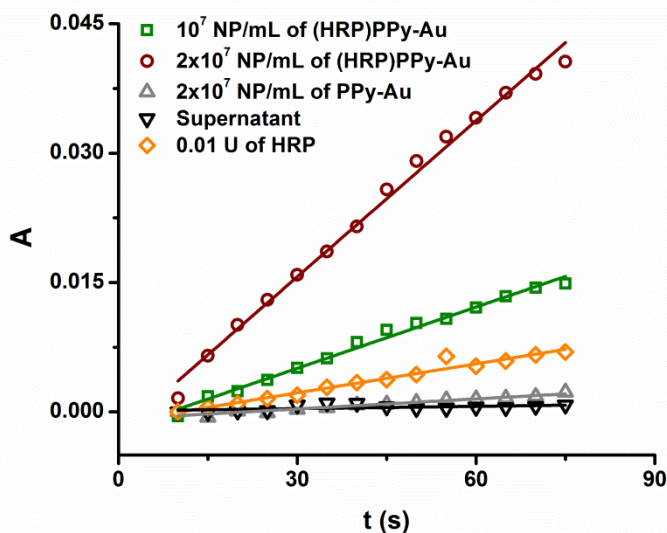


Figure 4S. The evolution of the absorbance at 620 nm for the supernatant recovered from the last of the washing steps following HRP immobilization (\blacktriangledown), PPy-Au nanorods not modified with HRP (\blacktriangle), 0.01 U of freely diffusing HRP (\blacklozenge), and two different concentrations of (HRP)PPy-Au nanorods (\blacksquare and \bullet). Observation: These evolutions of the absorbance clearly demonstrate that HRP is immobilized onto our nanorods and retains its peroxidase activity.

Colorimetric determination of peroxidase activity

Confirming that our protein immobilization methods are working was obviously important. Therefore, the immobilization of HRP onto the gold or PPy segments was spectrophotometrically confirmed. In order to determine the enzymatic activity of immobilized HRP we used a TECAN Infinite F200 Pro plate reader and NUNC 48-well plates. In each well we prepared a mixture of 1335 μL of water, 15 μL of phosphate buffer with a pH of 6.0, 25 μL of nanomotor suspension or enzyme stock solution, and 25 μL of an aqueous tetramethylbenzidine solution (0.5%, used as co-substrate and color reagent). The experimental protocol carried out by the computer-controlled plate reader consisted in shaking the mixture, followed by the injection of 100 μL of a 1.5% solution of hydrogen peroxide and further shaking. The absorbance of the mixture was measured every five seconds at 620 nm for 75 seconds. Every enzymatic assay consisted in determining the absorbance of two concentrations of HRP-modified nanorods, unmodified nanorods, supernatant recovered from the washing steps following HRP immobilization, and at least one sample with an enzyme stock solution of a known concentration (as shown also in Figure 4S).

Determination of the diffusion coefficient of the nanorods

Particles, moving in solutions with different concentrations of hydrogen peroxide (0-100 mM), were filmed about 20 hours after finishing enzyme immobilization. The films were made using an Axio Observer D1 microscope (from Carl Zeiss), a DfX 31AF03 camera (from The Imaging Source), and the Lucam Recorder software (version 2.7, from www.astrofactum.de). Each film consisted of 250 frames recorded at a speed of 15 frames per second (see typical film as an MP4 file in the Supplementary Information section). Icy software (version 1.2.7.0) was subsequently used to detect and then track particles in these movies³. This software also has an incorporated script which computes mean-squared displacements (MSDs) for the detected and tracked particles. The slope of the MSD vs. time interval representation was used to calculate the diffusion coefficient of the particles as previously described⁴. In order to easily compare the diffusive movement of particles which have different sizes, the diffusion coefficients of the particles in hydrogen peroxide solutions are presented as the relative difference from the coefficient of the same particles in water. All seven nanorod structures listed in Table 1 were fabricated, and subsequently tested, three times. The movement of at least 25 nanorods (from at least 6 different areas of the same sample) was analyzed for every hydrogen peroxide concentration and every particle batch. Therefore, the results presented are from the analysis of more than 3600 particles in different experimental conditions. Every diffusion coefficient reported is the result of tracking at least 75 particles in similar conditions.

Tests were also conducted to see the effect of time on the diffusion coefficient in hydrogen peroxide solutions (i.e. to see whether the observed increase of the diffusion coefficient is transient or not) (see Figure 5S).

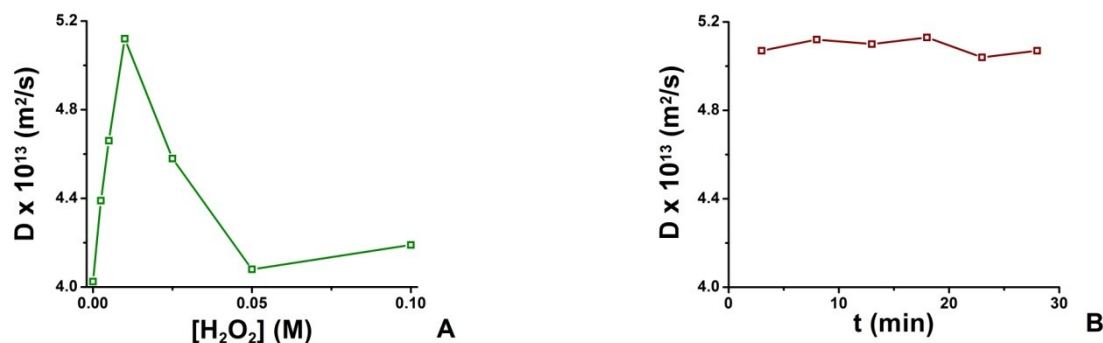


Figure 5S. Variation of the absolute diffusion coefficient of (HRP)PPy-Au nanorods with hydrogen peroxide concentration (A) as well as with time at a constant concentration of 10 mM hydrogen peroxide (B). Observation: Time has little impact on the diffusion coefficient as compared to the effect of hydrogen peroxide on the diffusion coefficient.

Figure 5S shows, the variation in diffusion coefficients for (HRP)PPy-Au nanorods in various hydrogen peroxide concentrations and also the variation of the diffusion coefficient for the same nanorods in 10 mM hydrogen peroxide over 30 minutes. The diffusion coefficient variation over this period of time is not significant as compared to the variation of the diffusion coefficient with the hydrogen peroxide, which is encouraging for the future applications of our nanorods (in sensing, for example).

Determination of the open circuit potential of the nanorod segments

In order to determine the open circuit potential of each nanorod segment (OCP_{segment}) in both water and hydrogen peroxide, the segments (i.e. their chemistries) were reproduced on gold electrodes by modifying 800 μm diameter gold wires with self-assembled monolayers of alkanethiols (or polypyrrole) and hemeproteins, just as described above for the nanorods. The open circuit potential of the modified electrodes was then determined versus a reference electrode (Ag/AgCl, 3M KCl), in water and 10 and 100 mM hydrogen peroxide using a VSP potentiostat from Bio-Logic SAS. Figure 6S shows the signal recorded in a typical experiment for the determination of the open circuit potential.

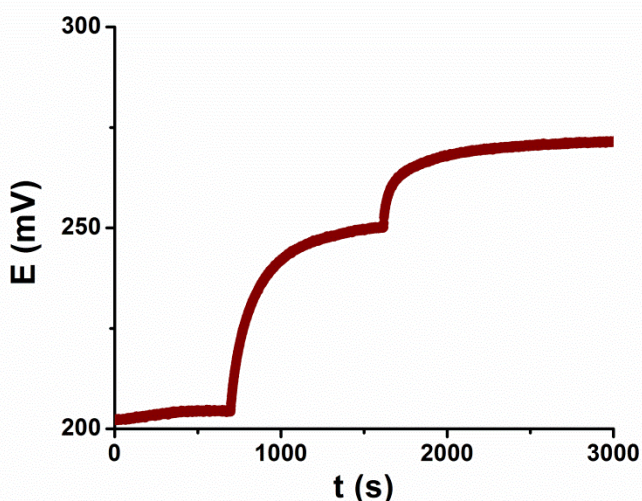


Figure 6S. Evolution of the open circuit potential for an electrode reproducing the chemistry of the Cyt c-modified gold segments of our nanorods. Once a stable open circuit potential was observed in water, the concentration of the hydrogen peroxide was increased to 10 mM (at $t = 698$ s) and subsequently to 100 mM (at $t = 1618$ s). Observation: Such measurements were made for all nanorod segments. The obtained OCP_{segment} values were then used to determine the open circuit potential difference characterizing each nanorod, $\Delta OCP_{\text{nanorod}}$.

Catalytic cycles of hemeproteins

HRP, Cat, and Cyt c are hemeproteins which convert hydrogen peroxide in several ways, depending on the experimental conditions. This is among the reasons why we have selected these proteins for our study. All the used hemeproteins were reported to have catalase activity (depicted in the upper part of Figure 7S) when only hydrogen peroxide is present as substrate (i.e. in the conditions of our experiments)⁵⁻⁷. All the used hemeproteins were also reported to have peroxidase activity⁸⁻¹¹. However, our experimental conditions do not supply reducing co-substrate (e.g. phenols or aromatic amines) for the hemeproteins to have full peroxidase-like catalytic cycles. Full peroxidase-like catalytic cycles are still possible if the hemeproteins accept electrons from the nanorods. All the used hemeproteins were reported to allow direct electron transfer to / from solid substrates (electrodes)¹²⁻¹⁷. This is another reason why we have selected these proteins for our study. As a consequence, peroxidase-like activity of the hemeproteins is also possible in our experimental conditions as long as the nanorods can supply electrons to the hemeproteins (as depicted in the lower part of Figure 7S).

Catalase activity of heme proteins on our nanorods:

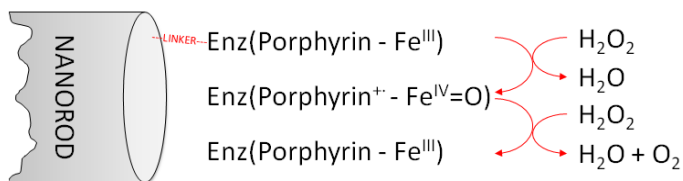
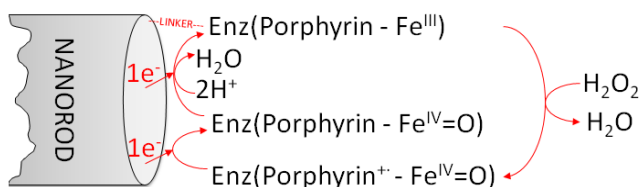


Figure 7S. Catalase-like activity (upper part) and peroxidase-like activity (lower part) of heme proteins immobilized onto nanorods.

Observation: In the absence of a reducing co-substrate peroxidase-like catalytic cycles are only possible by accepting electrons from the nanorod.

Peroxidase activity of heme proteins on our nanorods:



References

1. B. R. Martin, D. J. Dermody, B. D. Reiss, M. Fang, L. A. Lyon, M. J. Natan, and T. E. Mallouk, *Adv. Mater.*, 1999, **11**, 1021–1025.
2. C. A. Schneider, W. S. Rasband, and K. W. Eliceiri, *Nat. Methods*, 2012, **9**, 671–675.
3. F. de Chaumont, S. Dallongeville, N. Chenouard, N. Hervé, S. Pop, T. Provoost, V. Meas-Yedid, P. Pankajakshan, T. Lecomte, Y. Le Montagner, T. Lagache, A. Dufour, and J.-C. Olivo-Marin, *Nat. Methods*, 2012, **9**, 690–696.
4. G. Dunderdale, S. Ebbens, P. Fairclough, and J. Howse, *Langmuir*, 2012, **28**, 10997–11006.
5. J. Hernandez-Ruiz, M. B. Arnao, A. N. Hiner, F. Garcia-Canovas, and M. Acosta, *Biochem. J.*, 2001, **354**, 107–114.
6. J. Vlasits, C. Jakopitsch, M. Bernroitner, M. Zamocky, P. G. Furtmueller, and C. Obinger, *Arch. Biochem. Biophys.*, 2010, **500**, 74–81.
7. N. Tomášková, L. Varinská, and E. Sedláč, *Gen. Physiol. Biophys.*, 2010, **29**, 255–265.
8. V. D. Artemchik, V. P. Kurchenko, and D. I. Metelitsa, *Biokhimiia Mosc. Russ.*, 1985, **50**, 1183–1188.
9. E. Horozova, N. Dimcheva, and Z. Jordanova, *Z. Naturforschung C- J. Biosci.*, 1998, **53**, 863–866.
10. R. E. M. Diederix, M. Ubbink, and G. W. Canters, *Biochemistry (Mosc.)*, 2002, **41**, 13067–13077.
11. N. H. Kim, M. S. Jeong, S. Y. Choi, and J. H. Kang, *Bull. Korean Chem. Soc.*, 2004, **25**, 1889–1892.
12. Y. Xiao, H. X. Ju, and H. Y. Chen, *Anal. Biochem.*, 2000, **278**, 22–28.
13. M. E. Lai and A. Bergel, *Bioelectrochemistry*, 2002, **55**, 157–160.
14. Y. T. Kong, M. Boopathi, and Y. B. Shim, *Biosens. Bioelectron.*, 2003, **19**, 227–232.
15. L. Wang and E. K. Wang, *Electrochem. Commun.*, 2004, **6**, 49–54.
16. J. Di, M. Zhang, K. Yao, and S. Bi, *Biosens. Bioelectron.*, 2006, **22**, 247–252.
17. J.-F. Wu, M.-Q. Xu, and G.-C. Zhao, *Electrochem. Commun.*, 2010, **12**, 175–177.